KSME

Springer

Journal of Mechanical Science and Technology 34 (8) 2020

Original Article
DOI 10.1007/s12206-020-0739-6

Keywords:
· Thermal storage type heat exchanger
· Double shell and tube
· Three heat transfer medium
· Phase change material (PCM)
· Heat storage

Correspondence to:
Chaedong Kang
ckang@jbnu.ac.kr

Citation:
Lee, D., Kang, C. (2020). Evaluation of heat storage and release in a double shell and tube heat exchanger with a PCM layer. Journal of Mechanical Science and Technology 34 (8) (2020) 3471~3480. http://doi.org/10.1007/s12206-020-0739-6

Received February 19th, 2020
Revised May 25th, 2020
Accepted June 11th, 2020

† Recommended by Editor Yong Tae Kang

Evaluation of heat storage and release in a double shell and tube heat exchanger with a PCM layer

Donggyu Lee[1] and Chaedong Kang[2,3]

[1]Corp Research Institute, SUN E&C Co., Ltd., Jeonju-si 54956, Korea, [2]Dept. of Mechanical Engineering, Jeonbuk National University, Jeonju-si 54596, Korea, [3]Geothermal Energy Technology Research Center, Jeonbuk National University, Jeonju-si 54596, Korea

Abstract In this study, a thermal storage type heat exchanger that combines heat storage and heat exchange functions has proposed and the heat transfer characteristics of the new type of heat exchanger were analyzed through experiments. The proposed thermal storage type heat exchanger has a shell and tube structure and allows mutual heat transfer between three or more mediums, including a phase change material (PCM). This thermal storage type heat exchanger contains 52.2 kg of a PCM with a phase change temperature of 68.8 °C to provide heat storage function. The heat transfer experiment of the heat exchanger confirmed the effect of the temperature change of the heating medium under the same flow conditions. Furthermore, due to the structural characteristics of the thermal storage type double shell and tube heat exchanger (TSDHE), the phenomenon of three-medium heat exchange (hot water-cold water, hot water-PCM, additional water-PCM) was verified during the experimental process. In particular, due to the PCM filled inside the heat exchanger, the cold water received a heat transfer of 3 kW or higher from the PCM for at least 5 min (maximum 33 min), even when the hot water supply (heat source) was stopped. The results of this study will be used as basic data for applying a thermal storage type evaporator to a high temperature heat pump that generates steam using industrial waste heat.

1. Introduction

Interest in unused energy has been increasing recently regions as strive toward efficient energy use and reduction of carbon dioxide emissions [1, 2]. Industrial waste heat (40~80 °C), which is a representative unused energy, is generated in the processes of power generation, food, and fiber industries. Technologies to efficiently recover industrial waste heat have been developed [3, 4], and networks have been constructed to use recovered energy [5]. In particular, industrial waste heat has been combined with heat pump systems to increase waste heat utilization efficiency and energy density [6, 7].

However, heat recovery system requires a stable waste heat supply, as waste heats generated in Industrial processes undergo qualitative and quantitative changes with time [8]. Especially, unstable heat sources in large heat pump systems lead to compressor damage and not comply with the rated operating conditions which results in lowering the system operating efficiency. Therefore, the use of industrial waste heat as a heat pump source requires providing a device for securing the stability of the heat source.

Heat source systems for air conditioning and industry typically include various types of heat exchanger [8-14] and heat storage tanks [15-19]. In particular, heat storage systems are often used as a means to solve the problems of systems using industrial waste heat. With regard to heat transfer in the PCM filling layer, almost all of the previous papers identify the phase change characteristics of the simple PCM filling layer due to two heat mediums (PCM layer around the coil or PCM in the capsule) [20-23]. Although there are studies using two PCMs, one PCM directly relates to a circulating heat medium.

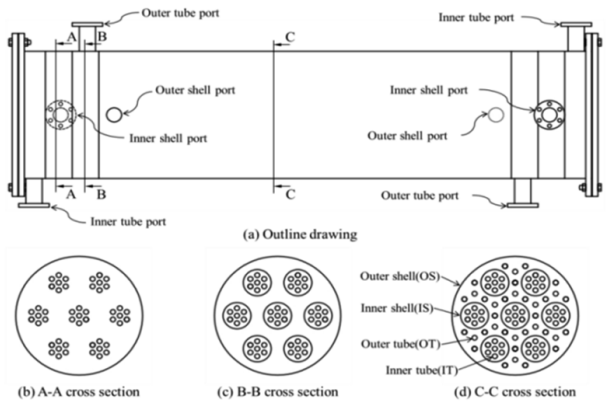

Fig. 1. Structure of the double shell and tube type heat exchanger.

In order to improve the unstable transient heat response that can occur when industrial waste heat is used as a heat source for a heat pump, a thermal storage type heat exchanger has been proposed in previous study [24]. Unlike the existing plate type (TSPHE; thermal storage type plate heat exchanger), we propose a new type of heat storage heat exchanger that has a shell and tube type as the basic structure. Therefore, the heat storage and release characteristics of the newly proposed thermal storage type heat exchanger were investigated through experimental methods.

2. Double shell and tube heat with PCM layer

Shell and tube heat exchangers, which account for more than 60 percent of all industrial heat exchangers, are low priced, easy to maintain, and can be produced in various sizes. A thermal storage type heat exchanger that combines a thermal storage tank and a heat exchanger were newly designed by modifying the existing structure of a shell and tube heat exchanger. Fig. 1 shows the outline and cross sectional view of the newly designed thermal storage type heat exchanger. In this study, the newly designed thermal storage type heat exchanger was named the TSDHE (thermal storage type double shell and tube heat exchanger). The TSDHE is composed of two pairs of shell and tube. Thus, the TSDHE has four flow channels and can mix different types of mediums in various ways in accordance with the desired application.

In TSDHE, one flow channel (outer shell) in the TSDHE was enclosed and filled with PCM to use as a heat exchanger with heat storage function. Furthermore, among the mediums used in the thermal storage type heat exchanger, that playing the role of heat supply source (hot water) flows in the inner shell, and the lowest temperature medium (cold water) flows in the inner tube. The PCM filling the outer shell exchanges heat with the mediums that flow in the outer tube and inner shell. However, the PCM filling the outer shell only changes its phase (solid↔liquid) without flowing. The thermal energy of the medium flowing in the inner shell is transmitted to the medium flowing in the inner tube, and part of it is sent to the PCM filling the outer shell for storage. The medium flowing in the outer tube is used to accelerate the melting process (heat storage process) of the PCM in the outer shell. In addition, the distances between the inner shell and outer tube and between the outer tubes were minimized in order to avoid an increase in the thermal resistance of the heat transfer surface that occurs during the phase change of the PCM from liquid to solid in the TSDHE. Fig. 2 shows a prototype of the TSDHE.

Fig. 2. Photograph of the actual prototype of TSDHE.

3. Experimental apparatus and method

Fig. 3 shows the experimental setup, which consists of constant temperature water tanks, a brine chiller (SJ-7.5AH, 7.5RT, air cooling), TSDHE, and pipe systems. For the experiment, the waste heat water was replaced with tap water, and the refrigerant was replaced with brine to form a heat medium. The TSDHE was placed in a standing position with supports, and heat loss was reduced by installing 50 mm thick nitrile butadiene rubber insulation. At the inlet and outlet for each medium, temperature, pressure, and flow sensors were installed. Temperature was measured using a K-type thermocouple, and the flow rate was measured using a turbine type flow meter. The measured data were stored on a PC using the Lab View® program. Table 1 shows the uncertainty of each measuring device and corresponds to the measuring range. Fig. 4 is a

photograph of the experimental device.

The phase change process of the PCM is difficult to observe with a naked eye because it locates in a closed space inside the heat exchanger. The phase change process of the PCM was checked by measuring the temperature inside the PCM. The temperature was measured at four points (height from the bottom: TP.1: 1.25 m, TP.2: 1 m, TP.3: 0.75 m, TP.4: 0.5 m) in 90° intervals on the same radius from the central axis inside the PCM area and perpendicular to the PCM layer (height: 0.89 m). The maximum amount of PCM that can be fill the outer shell of the TSDHE fabricated for this study is 54 kg, but only 52.2 kg (approximately 96.7 %) was added considering PCM volume expansion. Table 2 lists the detailed thermal properties of the PCM.

The experiment can be divided into three processes: heat storage, simultaneous heat storage and release, and heat release. In the heat storage process, with the cold water stopped, hot water was circulated until the solid state PCM in the heat exchanger was fully melted by changing the hot water supply temperature between the constant temperature water tank and heat exchanger. In the simultaneous heat storage and release process, at the moment when the heat storage process finished, with the hot water circulating, the cold water was circulated so that heat storage and release would occur simultaneously. Lastly, in the heat release process, the hot water supply was stopped assuming abnormal operation where the heat supply is stopped, and only cold water was circulated until the liquid state PCM in the heat exchanger was fully solidified.

Table 3 lists the operation conditions for each experimental process. The heat transfer rate in the heat exchanger of each medium at each operation condition was calculated by applying the instantaneous temperatures at the inlet and outlet of the heat exchanger for each medium and the instantaneous flow rate measured at the inlet of the heat exchanger. In addition, the average heat transfer rate was determined by dividing the sum of the instantaneous heat transfer rates by the total process time as shown in Eq. (1). And the heat capacities of each heat medium are as shown in Eq. (2).

Table 1. Measurement devices and their uncertainties.

Instruments	Type	Range	Accuracy
Temperature	K-type thermocouples	-50~500 °C	±0.1 °C
Flow meter	Turbine type	0.1~1.2 CMH	±0.5 % of full scale
Data acquisition	NI cDAQ-9174	-	-

$$\dot{Q}_{A,m} = \frac{1}{t - t_0}\int_{t=0}^{t} \dot{Q}_A dt \tag{1}$$

$$Q_{A,m} = \dot{Q}_{A,m}\left(t_f - t_0\right) \tag{2}$$

$$A:\ h\ (hot\ water),\ c\ (cold\ water),\ a\ (additional\ water).$$

The capacity of heat storage and heat release by the PCM in the heat exchanger through heat storage and release proc-

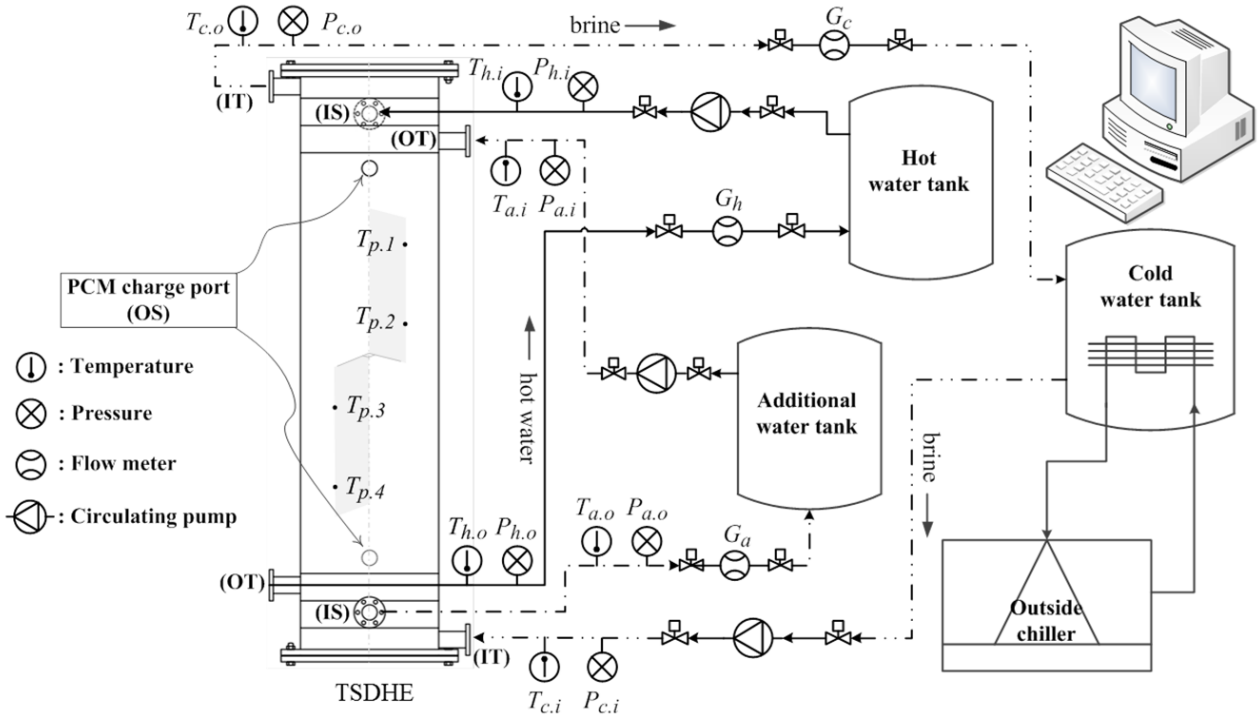

Fig. 3. Schematic diagram of the experimental device.

Table 2. Thermal properties of the phase change material (PCM) (at 25 °C, by the KITECH).

Item	Value
Melting point [°C]	68.8
Latent heat [kJ/kg]	198.8
Density [kg/m^3]	940
Specific heat [kJ/kg·K]	2.83
Viscosity [N·s/m^2]	3.90×10^{-3}
Thermal conductivity [W/m·K]	0.29

Table 3. Experimental conditions for heat storage and release in the TSDHE.

Passes	Heat media	T_i [°C]			G [LPM]		
		HS	HR	HSR	HS	HR	HSR
Inner tube	Brine	-	40	40	-	2	2
Inner shell /outer tube	Water	70~90	-	70~90	10	-	10
Outer shell	PCM	-	-	-	-	-	-

(HS: heat storage only, HR: heat release only, HSR: heat storage-release simultaneously)

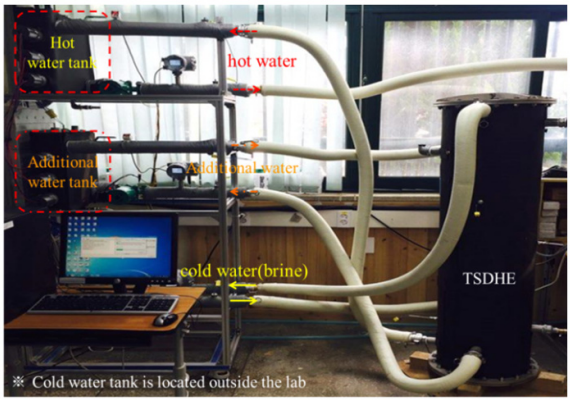

Fig. 4. Picture of the configured experimental device.

esses were calculated by Eq. (3).

$$Q_{P,m} = \left(Q_{h,m} - Q_{c,m} + Q_{a,m}\right). \tag{3}$$

Then, the heat storage ratio in the PCM during the simultaneous heat storage and release process was calculated as shown by Eq. (4).

$$R = \frac{Q_{P,m}}{\left(Q_{h,m} + Q_{a,m}\right)}. \tag{4}$$

In each experimental condition, all analytical values were obtained at 6 times more by averaging the values measured at steady state.

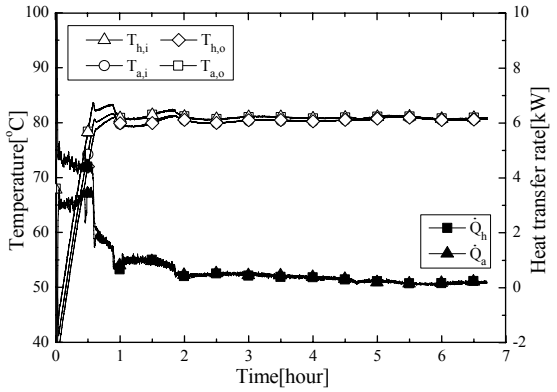

Fig. 5. Time variations in inlet/outlet temperature and heat transfer rate during heat storage ($T_{h,i}$ = $T_{a,i}$ = 80 °C, G_h = G_a = 10 LPM, G_c = 0 LPM).

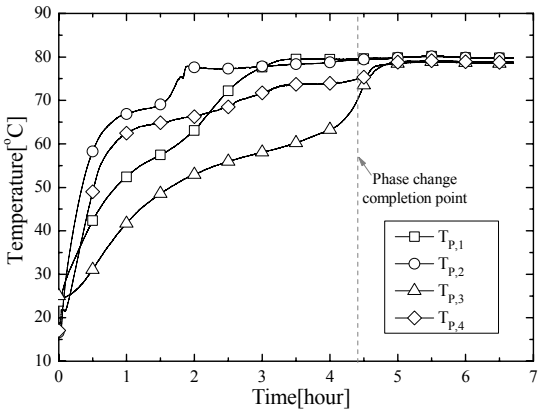

Fig. 6. Time variation of temperature of the PCM layer during the heat storage process ($T_{h,i}$ = $T_{a,i}$ = 80 °C, G_h = G_a = 10 LPM, G_c = 0 LPM).

4. Results and discussions

4.1 Heat storage characteristics of the TSDHE

Fig. 5 shows one of the heat storage conditions in Table 3 when hot water (used instead of industrial waste heat water) at 10LPM and 80 °C is supplied to the inner shell and outer tube without brine supply to the inner tube. It shows the change hot water inlet temperature, outlet temperature, and heat transfer rate of the TSDHE over time. In response to hot water supply temperature, the heat transfer rates on the inner shell side and the outer tube side in the first 40 minutes were high at 5.49 kW and 3.60 kW, respectively. However, after five hours, both heat transfer rates were at 0.5 kW or lower. There is slight heat transfer in TSDHE because the heat is fully stored to PCM, i.e., thermal equilibrium occurs inside TSDHE and no further heat exchange occurs.

Fig. 6 shows the temperature variation inside the PCM in the outer shell during the experiment described in Fig. 5 with the supply of working fluid, the PCM temperature in the heat exchanger increased sharply from the initial temperature of 22 °C, passed through the phase change point (68.8 °C), and reached equilibrium at around 80 °C. It is not easy to determine the exact time when the PCM changed from the initial solid state to

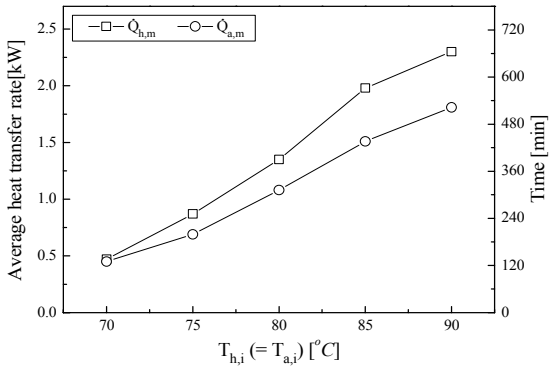

Fig. 7. Average heat transfer rate of working fluids during the heat storage process (G_h = G_a = 10 LPM, G_c = 0 LPM).

liquid. However, the inflection point of the temperature curve generally occurs near the end of the PCM phase change, and the phase change can be determined based on this point.

Hence, the time of the second inflection point of the temperature curve of the bottom measurement point in the temperature trend line was assumed to be the rough phase change end point (= heat storage ending). As a result, it took approximately four hours 30 min for complete melting of the PCM. Furthermore, the average heat transfer rate of the working fluid during the heat storage process was 1.35 kW on the hot water side (inner shell) and 1.08 kW on the additional water side (outer tube).

Fig. 7 outlines the results for the heat storage process among the experimental conditions listed in Table 3. For each experimental condition, the average heat transfer rate was analyzed. As the temperature of the hot water side (inner shell, outer tube) increased, the average heat transfer rate to the PCM increased. Moreover, the hot water in the inner shell was more effective at melting the PCM than that in the outer tube (additional water). Table 4 shows the measurement uncertainty for the results in Fig. 7.

Fig. 8 shows the thermal storage capacity and storage end time during the heat storage process. As the hot water supply temperature ($T_{h,i} = T_{a,i}$) increases, the storage end time decreases. Also, the highest heat storage capacity was shown when the hot water supply temperature ($T_{h,i} = T_{a,i}$) was 80 °C. The heat storage capacity slightly decreased when the hot water supply temperature ($T_{h,i} = T_{a,i}$) was above 80 °C, but remained above a certain level. It is considered that the heat loss increased with the increase in the hot water supply temperature ($T_{h,i} = T_{a,i}$) in the state where the thickness of the insulation surrounding the TSDHE was constant. However, as the hot water supply temperature ($T_{h,i} = T_{a,i}$) increases, the heat storage speed is observed to increase.

4.2 Simultaneous heat storage and release characteristics of the TSDHE

Fig. 9 shows the changes in inlet and outlet temperatures and heat transfer rate of the working fluid when simultaneous

Table 4. Measurement uncertainty of $\dot{Q}_{a,m}$ and $\dot{Q}_{h,m}$ in the heat storage process.

Condition ($T_{h,i} = T_{a,i}$) [°C]	Uncertainties in measurement	
	$\dot{Q}_{a,m}$	$\dot{Q}_{h,m}$
70	(0.45±0.12) kW (C.L. about 95 %, k = 2.00)	(0.47±0.12) kW (C.L. about 95 %, k = 2.00)
75	(0.69±0.11) kW (C.L. about 95 %, k = 2.00)	(0.87±0.13) kW (C.L. about 95 %, k = 2.00)
80	(1.08±0.14) kW (C.L. about 95 %, k = 2.00)	(1.35±0.16) kW (C.L. about 95 %, k = 2.00)
85	(1.51±0.15) kW (C.L. about 95 %, k = 2.09)	(1.98±0.16) kW (C.L. about 95 %, k = 2.11)
90	(1.81±0.17) kW (C.L. about 95 %, k = 2.07)	(2.30±0.19) kW (C.L. about 95 %, k = 2.13)

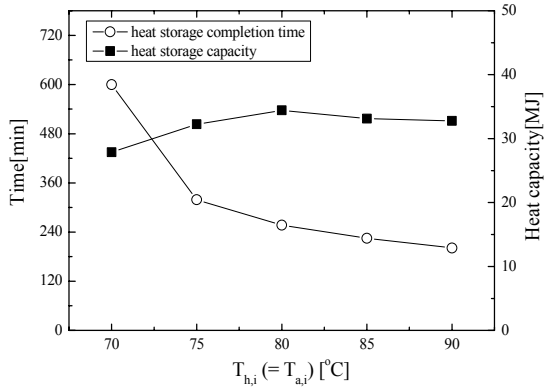

Fig. 8. Heat storage capacity and storage end time of the TSDHE during the heat storage process (G_h = G_a = 10 LPM, G_c = 0 LPM).

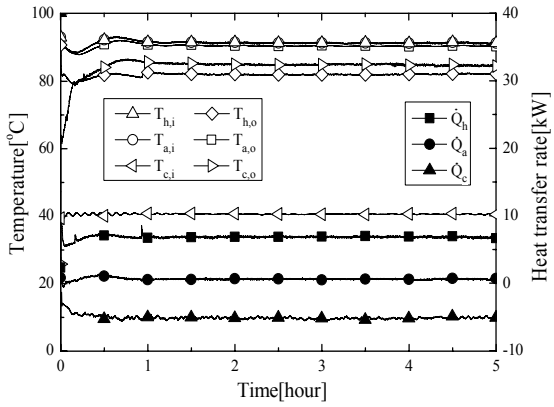

Fig. 9. Time variation in inlet/outlet temperatures and heat transfer rate during the simultaneous heat storage and release process ($T_{h,i}$ = $T_{a,i}$ = 90 °C, $T_{c,i}$ = 40 °C, G_h = G_a = 10 LPM, G_c = 2 LPM).

heat storage and release experiment was performed by additionally supplying cold water (brine) through the inner tube at the time of heat storage completion. Simultaneous heat storage and release is a process in which cold water (brine) is supplied through the inner tube, while hot water is supplied through the inner shell and outer tube. In the simultaneous

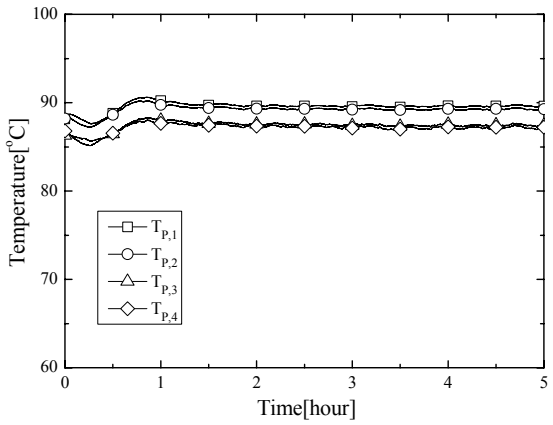

Fig. 10. Time variation in temperature of the PCM layer during the simultaneous heat storage and release process ($T_{h,i}$ = $T_{a,i}$ = 90 °C, $T_{c,i}$ = 40 °C, G_h = G_a = 10 LPM, G_c = 2 LPM).

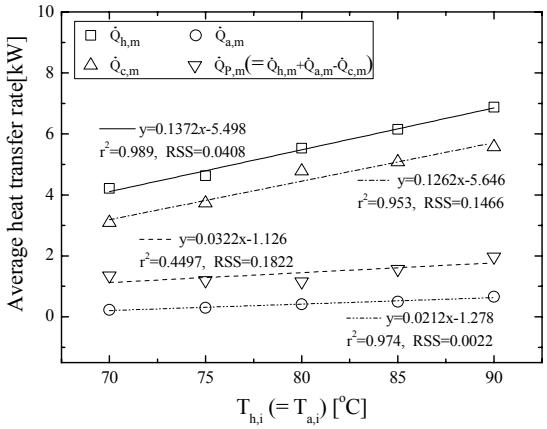

Fig. 11. The average heat transfer of working fluids during the simultaneous heat storage and release process ($T_{h,i}$ = $T_{a,i}$ = 90 °C, $T_{c,i}$ = 40 °C, G_h = G_a = 10 LPM, G_c = 2 LPM).

heat storage and release process, the thermal energy supplied through the hot water of the inner shell is sent to the cold water (brine) of the inner tube, and some surplus thermal energy is sent to the PCM stored in the outer shell. At this moment, the hot water supplied through the outer tube continuously transmits thermal energy to the PCM. Furthermore, depending on the temperature of the hot water supplied through the inner shell, the thermal energy stored in the PCM of the outer shell can be also sent to the cold water (brine) of the inner tube through the inner shell ($T_{P.melt} = T_h$).

As shown in Fig. 9, the heat exchanger was in a transient state for approximately 30 min after the experiment began, and then the temperature stabilized after showing slight fluctuations. In this process, the average heat transfer rate of each working fluid was 6.86 kW in hot water (inner shell), 0.603 kW in additional water (outer tube), and 5.163 kW in brine (inner tube). Furthermore, the average heat transfer rate to the PCM during the experimental process ($Q_{P.m}$) was approximately 2.3 kW.

Fig. 10 shows the temperature variation inside the PCM in the outer shell during the experimental process of Fig. 9. In the simultaneous heat storage and release process, hot water is continuously supplied through the outer tube. Thus, the temperature inside the PCM was higher than the phase change point (68.8 °C) as after the heat storage experiment was completed, and the PCM maintained a liquid state.

Fig. 11 shows analysis of experimental results for the simultaneous heat storage and release process among the experimental conditions listed in Table 3. The average heat transfer rate of every working fluid is summarized based on hot water supply temperature.

For example, when the hot water supply temperature was 70 °C, the heat transfer rate was 4.21 kW in the inner shell (hot water), 0.23 kW in the outer tube (additional water), and 3.09 kW in the inner tube (brine). The thermal energy transferred to the PCM layer was 1.35 kW by Eq. (3). In particular, as the hot water supply temperature increased, the total heat transfer rate ($\dot{Q}_{h.m} + \dot{Q}_{a.m}$) of the hot water also increased, but,

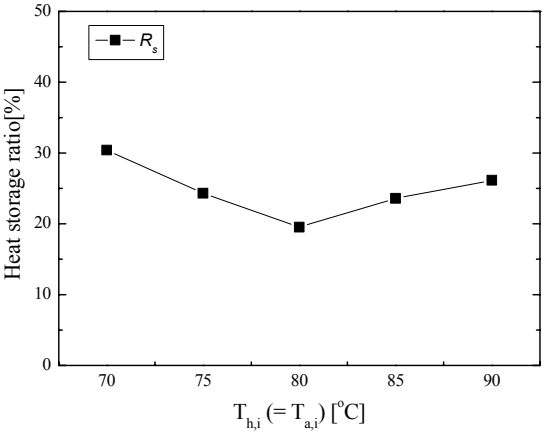

Fig. 12. Heat storage ratio in the simultaneous heat storage and release process ($T_{h,i}$ = $T_{a,i}$ = 90 °C, $T_{c,i}$ = 40 °C, G_h = G_a = 10 LPM, G_c = 2 LPM).

as the temperature difference between hot water and cold water increased, $\dot{Q}_{c.m}$ also increased proportionally. Nevertheless, in the simultaneous heat storage and release process, the PCM already finished the phase change and maintained a liquid state. Thus, the increase rates of $\dot{Q}_{a.m}$ and $\dot{Q}_{P.m}$ were smaller than those of $\dot{Q}_{h.m}$ and $\dot{Q}_{a.m}$.

Fig. 12 shows the heat storage ratio in the simultaneous heat storage and release process based on the experimental result in Fig. 11. The difference between heat storage and release was caused by the temperature of each heat medium. In general, as the temperature difference between two heating mediums increases, the heat transfer rate between mediums increases. However, the TSDHE affects not only the heat transfer rate, but also the heat transfer direction due to displacement of the three heat mediums. As shown in Fig. 12, the lowest heat storage ratio was obtained at the inlet temperature of 80 °C. This is due to the triple heat exchange between the three heat mediums due to the structural effect of TSDHE. When $T_{h,i}$ increase, the value of $\Delta T_{hc}\left(=T_h - T_c\right)$ and the value of $\Delta T_{hP}\left(=T_h - T_P\right)$ also increases. However, the in-

Table 5. Measurement uncertainty about R_s in the simultaneous heat storage and release process.

Conditions [°C] ($T_{h,i} = T_{a,i}$)	Measurement uncertainty
70	(30.4±3.3) % (C.L. about 95 %, *k* = 2.00)
75	(24.3±2.1) % (C.L. about 95 %, *k* = 2.09)
80	(19.5±2.0) % (C.L. about 95 %, *k* = 2.13)
85	(23.6±2.3) % (C.L. about 95 %, *k* = 2.00)
90	(26.1±1.9) % (C.L. about 95 %, *k* = 2.00)

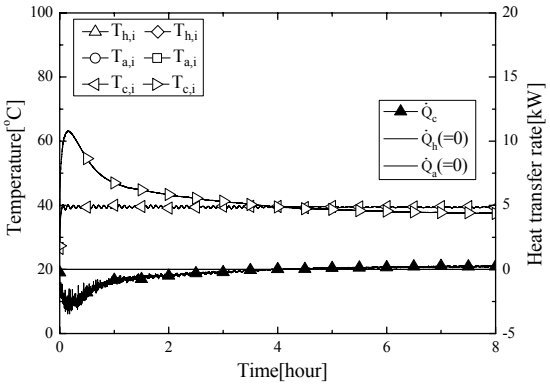

Fig. 13. Time variations in inlet/outlet temperatures and heat transfer rate during the heat release process ($T_{c,i}$ = 40 °C, G_h = G_a = 0 LPM, G_c = 2 LPM).

crease in $Q_{P,m}$ due to the increase in ΔT_{hP} is greater than the increase in $Q_{c,m}$ according to the increase in ΔT_{hc}, so it is estimated that the inlet temperature is 80 °C. And, the heat storage rate might be changed due to the TSDHE structure and the thermo physical characteristics of the PCM. Therefore, it was confirmed that the amount of heat stored in the PCM can be controlled by changing the inlet temperature of the hot side water. Table 5 shows the measurement uncertainty for the results in Fig. 12.

4.3 Heat release characteristics of the TSDHE

Fig. 13 shows the heat release process, i.e., temperature variation of working fluid in the TSDHE heat exchanger, when only cold water (brine) was supplied at approximately 40 °C with a flow rate of 2LPM through the inner tube, while the hot water supply was stopped after completion of the simultaneous heat storage and release experiment. In this study, the heat release process was defined as the state of supplying only cold water while stopping the hot water supply in the TSDHE. In the heat release process, the heat stored in the PCM filling the outer shell was released through the cold water (brine) in the inner tube. As shown in Fig. 13, the cold water (brine) outlet temperature in the beginning of the experiment sharply increased and then gradually decreased. Immediately after starting the experiment, the release heat transfer rate was 1.47 kW, but after reaching the maximum release heat transfer rate of

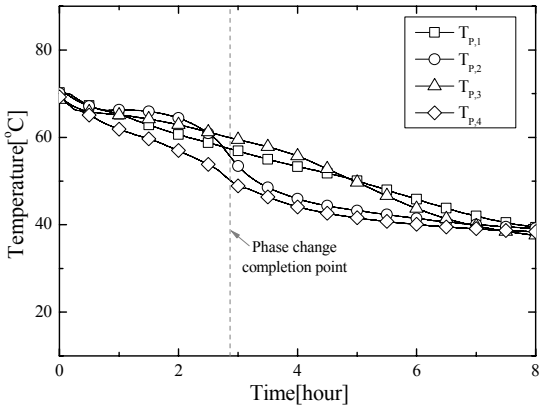

Fig. 14. Time variation of temperature of the PCM layer during the heat release process ($T_{c,i}$ = 40 °C, G_h = G_a = 0 LPM, G_c = 2 LPM).

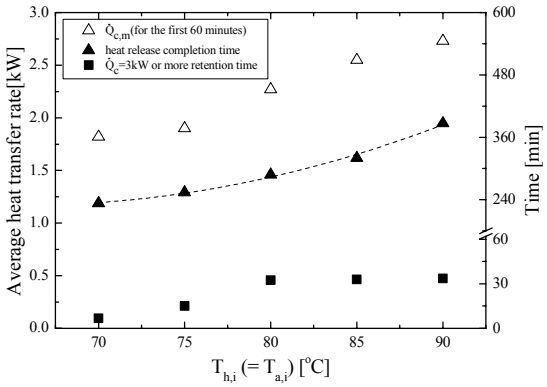

Fig. 15. Average heat transfer rate and heat release end time during the heat release process ($T_{c,i}$ = 40 °C, G_h = G_a = 0 LPM, G_c = 2 LPM).

3.35 kW, it gradually decreased.

Fig. 14 shows the temperature variation in the PCM contained in the outer shell during the experimental process of Fig. 13. The PCM was in liquid state before the experiment. As thermal energy was released through the cold water, the inside temperature of the PCM layer also gradually decreased. The time when the PCM became fully solidified was defined as the second inflection point of the decreasing temperature curve. Accordingly, in the experimental conditions of Figs. 13 and 14, the rapid heat release time was approximately 30 minutes, and the average release heat transfer rate during the about 3 hours of the final phase change was 1.82 kW.

Fig. 15 shows the analysis result of heat release end time and average heat transfer rate of the TSDHE heat exchanger during the heat release process given the experimental conditions listed in Table 3. After the simultaneous heat storage and release process was completed at a high hot water supply temperature ($T_{h,i} = T_{a,i}$), the release end time and the average heat transfer rate were high at the experimental conditions for heat release process. This suggests that the heat storage temperature of the TSDHE increased due to the high hot water supply temperature, and the heat storage increased. In particular, the heat transfer rate ($\dot{Q}_c$) stayed above 3 kW when the

Table 6. Measurement uncertainty about $\dot{Q}_{c,m}$ in the heat release process.

Conditions [°C] ($T_{h,i} = T_{a,i}$)	Measurement uncertainty
70	(1.82±0.21) kW (C.L. about 95 %, k = 2.25)
75	(1.91±0.23) kW (C.L. about 95 %, k = 2.28)
80	(2.27±0.16) kW (C.L. about 95 %, k = 2.20)
85	(2.55±0.13) kW (C.L. about 95 %, k = 2.17)
90	(2.73±0.09) kW (C.L. about 95 %, k = 2.11)

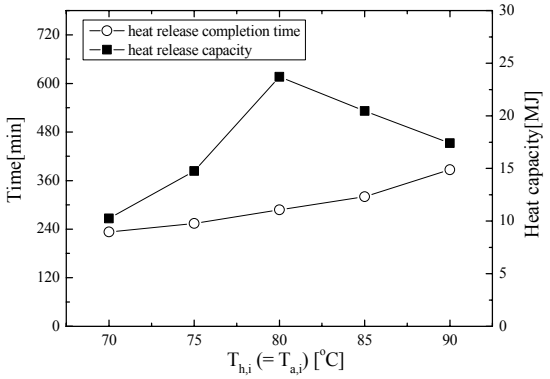

Fig. 16. The capacity and heat release time of the TSDHE during the heat release process ($T_{c,i}$ = 40 °C, G_h = G_a = 0 LPM, G_c = 2 LPM).

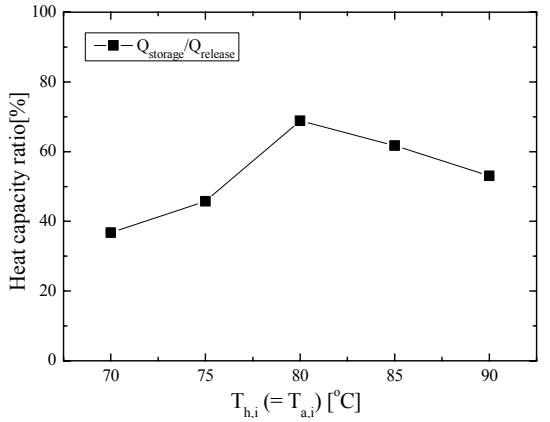

Fig. 17. Thermal capacity ratio of the TSDHE between heat storage and heat release.

hot water supply temperature was above 80 °C for more than 30 min. Table 6 shows the measurement uncertainty for the obtained results in Fig. 15.

Fig. 16 shows the heat release capacity and release end time during the heat release process. The higher the hot water supply temperature ($T_{h,i} = T_{a,i}$), the longer the heat release end time. However, the heat release capacity was also the highest because the highest heat storage capacity was obtained when the hot water supply temperature ($T_{h,i} = T_{a,i}$) was 80 °C in the results of Fig. 8. At this time, the heat release rate was the fastest when the hot water supplies temperature ($T_{h,i} = T_{a,i}$) was 80 °C.

4.4 Discussion

In this study, a basic experiment was conducted using a Thermal storage type heat exchanger that combines heat storage and heat exchange. The Thermal storage type heat exchanger includes a space for PCM for heat storage. Therefore, It showed different heat transfer characteristics than the existing heat exchanger. The phase change material filled inside the TSDHE was melted by the hot water and additional water and solidified by cold water. The TSDHE showed stable heat exchange characteristics after the PCM was completely melted. Unlike conventional heat exchangers, heat storage capacity and heat release capacity were analyzed to investigate the characteristics of thermal storage type heat exchanger combined with heat storage function.

Fig. 17 shows a comparison of the heat storage capacity during the heat storage process with the heat release capacity released during the heat storage process. The highest thermal capacity ratio was obtained when the hot water supply temperature ($T_{h,i} = T_{a,i}$) was 80 °C. This result is considered to occur in the difference between the phase change temperature and the heat capacity of the phase change material filled in the thermal storage type heat exchanger. This is due to a combination of problems, including heat loss to the surroundings, phase change inside the heat exchanger, heat exchange between the heat medium.

5. Conclusions

In this study, basic experiments were conducted within a lab scale heat exchanger, i.e., PCM containing a double shell and tube heat exchanger (TSDHE), newly designed by the authors for more efficient use of industrial waste heat. Two closed spaces in the TSDHE were filled with a phase change material (PCM). Then hot water and cold water were circulated, and the heat storage and release characteristics were verified through experiments. The following conclusions were obtained in this study.

(1) During the heat storage process and the simultaneous heat storage and release process, the average heat transfer rate by hot water was higher in the inner shell than in the outer tube.

(2) When the PCM was fully melted, in the simultaneous heat storage and release process in which hot water and cold water(brine) are supplied simultaneously, the average heat transfer rate of the cold water (brine) of the TSDHE was maintained at 5 kW or higher, and the average heat transfer rate of hot water also increased in proportion to the hot water supply temperature.

(3) In abnormal operation such that the hot water supply is interrupted can be used for 5~33 minutes a regenerative double and shell heat exchangers based on the PCM thermal stor-

age in the heat transfer rate of more than 3 kW.

Acknowledgments

This work was supported by (1) the Energy Demand Management Core Technology Development Project (10049090, Development of 300 kW high temperature heat pumps for steam supply up to 120 °C for industrial use) funded by the Ministry of Trade, Industry, & Energy (MOTIE, Korea) and (2) the Jeonbuk National University funds for domestic research (JBNU-09-2016).

Nomenclature

A : Heat transfer surface area, m^2
$C.L.$: Confidence level
C_p : Specific heat, kJ/kg·K
D : Diameter, mm
G : Volumetric flow rate, LPM
P : Pressure, kPa
Q : Heat transfer rate, kW
R : Heat storage ratio, %
T : Temperature, °C
k : Coverage factor
L : Length, m
$\dot{m}$: Mass flow rate, kg/s
t : Time, s

Subscripts

P : Phase change material (PCM)
a : Additional water
c : Cold water
f : Final
h : Hot water
i : Inlet
m : Average value
o : Outlet

References

[1] K. Park and S. Kim, Utilizing unused energy resources for sustainable heating and cooling system in buildings: A case study of geothermal energy and water sources in a university, *Energies*, 11 (7) (2018) 1836.

[2] N. C. Baek, U. C. Shin and J. H. Yoon, A study on the design and analysis of a heat pump heating system using wastewater as a heat source, *Solar Energy*, 78 (3) (2005) 427-440.

[3] H. Jouhara, N. Khordehgah, S. Almahmoud, B. Delpech, A. Chauhan and S. A. Tassou, Waste heat recovery technologies and applications, *Thermal Science and Engineering Progress* (2018).

[4] C. Chow and J. Duquette, Assessment of a heat pump based wastewater heat recovery system for a canadian university campus, *The Energy and Sustainability 2018 Symposium,* Springer, Cham. (2018) 146-167.

[5] H. W. Kim, L. Dong, A. E. S. Choi, M. Fujii, T. Fujita and H. S. Park, Co-benefit potential of industrial and urban symbiosis using waste heat from industrial park in Ulsan, Korea, *Resources, Conservation and Recycling*, 135 (8) (2018) 225-234.

[6] S. Garland, T. M. Bandhauer, A. Grauberger, J. Simon, D. Young, K. Eisemann and M. J. Reinke, Experimental investigation of a waste heat driven turbo compression chiller, *TFEC-2018* (2018).

[7] F. Meggers and H. Leibundgut, The potential of wastewater heat and exergy: Decentralized high temperature recovery with a heat pump, *Energy and Buildings*, 43 (4) (2018) 879-886.

[8] Z. Y. Xu, R. Z. Wang and C. Yang, Perspectives for low temperature waste heat recovery, *Energy*, 176 (2019) 1037-1043.

[9] S. Kakac, H. Liu and A. Pramuanjaroenkij, *Heat Exchangers: Selection, Rating, and Thermal Design*, CRC Press (2020).

[10] T. Tinker, Shell side characteristics of shell and tube heat exchangers, *General Discussion on Heat Transfer* (1951) 89-116.

[11] S. V. Patankar and D. B. Spalding, *A Calculation Procedure for the Transient and Steady State Behaviour of Shell-and-tube Heat Exchangers*, Department of Mechanical Engineering, Imperial College of Science and Technology (1972).

[12] W. W. Focke, J. Zachariades and I. Olivier, The effect of the corrugation inclination angle on the thermohydraulic performance of plate heat exchangers, *International Journal of Heat and Mass Transfer*, 28 (8) (1985) 1469-1479.

[13] M. K. Bassiouny and H. Martin, Flow distribution and pressure drop in plate heat exchangers—I U-type arrangement, *Chemical Engineering Science*, 39 (4) (1984) 693-700.

[14] D. G. Prabhanjan, G. S. V. Raghavan and T. J. Rennie, Comparison of heat transfer rates between a straight tube heat exchanger and a helically coiled heat exchanger, *International Communications in Heat and Mass Transfer,* 29 (2) (2002) 185-191.

[15] Y. Park and K. Kim, A study on the horizontal ground source heat pump greenhouse heating system with thermal storage tank, *Journal of Energy Engineering*, 15 (3) (2006) 194-201.

[16] S. H. Oh, R. Yun and Y. Cho, Studies on raw water source heat pump equipped with thermal storage tank in water treatment facility, *Trans. Korean Soc. Mech. Eng. B*, 37 (5) (2013) 467-472.

[17] Z. Lavan and J. Thompson, Experimental study of thermally stratified hot water storage tanks, *Solar Energy*, 19 (5) (1977) 519-524.

[18] Y. H. Zurigat, P. R. Liche and A. J. Ghajar, Influence of inlet geometry on mixing in thermocline thermal energy storage, *International Journal of Heat and Mass Transfer*, 34 (1) (1991) 115-125.

[19] E. M. Kleinbach, W. A. Beckman and S. A. Klein, Performance study of one dimensional models for stratified thermal storage tanks, *Solar Energy*, 50 (2) (1993) 155-166.

[20] J. P. Da Cunha and P. Eames, Thermal energy storage for low and medium temperature applications using phase change materials - A review, *Applied Energy*, 177 (2016) 227-238.

[21] Y. T. Lee, M. H. Kim, S. S. Lee, J. Gim and J. D. Chung, Numerical analysis in a full-scale thermal energy storage tank with dual PCM capsules, *Energy & Buildings,* 204 (2019) 109410.
[22] J. C. Kurnia, A. P. Sasmito, S. V. Jangam and A. S. Mujumdar, Improved design for heat transfer performance of a novel phase change material (PCM) thermal energy storage (TES), *Applied Thermal Engineering,* 50 (2013) 896-907.
[23] M. Y. Abdelsalam, P. Sarafraz, J. S. Cotton and M. F. Lightstone, Heat transfer characteristics of a hybrid thermal energy storage tank with phase change materials (PCMs) during indirect charging using isothermal coil heat exchanger, *Solar Energy*, 157 (2017) 462-476.
[24] D. Lee and C. Kang, A study on development of the thermal storage type plate heat exchanger including PCM layer, *Journal of Mechanical Science and Technology*, 33 (12) (2019) 6085-6093.

Donggyu Lee received B.S. and M.S. degrees in Mechanical Engineering from Jeonbuk National University in 2006 and 2008. And, he went on to earn doctoral of engineering from the same university in 2015. His research interests are in the areas of refrigeration, HVACs, ice storage systems, geothermal energy system. In recent years, he has been studying heat exchanger that combines thermal storage and heat exchange function using phase change materials.

Chaedong Kang received a B.S. degree in Mechanical Engineering from Kyunghee University in 1985 and an M.S. degree in Mechanical Engineering from KAIST in 1989. He then went on to earn his Dr. Eng. degree from the Tokyo Institute of Technology in 1997. Dr. Kang is currently an Associate Professor of the Department of Mechanical Engineering at Jeonbuk National University in Jeonju, Korea. His research interests are in the areas of refrigeration, building HVACs, ice storage systems, and molecular simulation.